

Beam-energy and system-size dependence of the space-time extent of the pion emission source produced in heavy ion collisions

- A. Adare,¹³ S. Afanasiev,³² C. Aidala,^{14, 41, 45, 46} N.N. Ajitanand,⁶⁴ Y. Akiba,^{58, 59} R. Akimoto,¹² H. Al-Bataineh,⁵² H. Al-Ta'ani,⁵² J. Alexander,⁶⁴ M. Alfred,²⁵ A. Angerami,¹⁴ K. Aoki,^{37, 58} N. Apadula,^{30, 65} L. Aphecetche,⁶⁶ Y. Aramaki,^{12, 58} R. Armendariz,⁵² S.H. Aronson,⁷ J. Asai,⁵⁹ H. Asano,^{37, 58} E.C. Aschenauer,⁷ E.T. Atomssa,^{38, 65} R. Averbeck,⁶⁵ T.C. Awes,⁵⁴ B. Azmoun,⁷ V. Babintsev,²⁶ M. Bai,⁶ G. Baksay,²⁰ L. Baksay,²⁰ A. Baldissari,¹⁶ N.S. Bandara,⁴⁵ B. Bannier,⁶⁵ K.N. Barish,⁸ P.D. Barnes,^{41, *} B. Bassalleck,⁵¹ A.T. Basye,¹ S. Bathe,^{5, 8, 59} S. Batsouli,⁵⁴ V. Baublis,⁵⁷ C. Baumann,⁴⁷ S. Baumgart,⁵⁸ A. Bazilevsky,⁷ M. Beaumier,⁸ S. Beckman,¹³ S. Belikov,^{7, *} R. Belmont,^{46, 70} R. Bennett,⁶⁵ A. Berdnikov,⁶¹ Y. Berdnikov,⁶¹ A.A. Bickley,¹³ X. Bing,⁵³ D. Black,⁸ D.S. Blau,³⁶ J.G. Boissevain,⁴¹ J. Bok,⁵² J.S. Bok,⁷⁴ H. Borel,¹⁶ K. Boyle,^{59, 65} M.L. Brooks,⁴¹ J. Bryslawskyj,⁵ H. Buesching,⁷ V. Bumazhnov,²⁶ G. Bunce,^{7, 59} S. Butsyk,^{41, 51, 65} C.M. Camacho,⁴¹ S. Campbell,^{30, 65} P. Castera,⁶⁵ B.S. Chang,⁷⁴ J.-L. Charvet,¹⁶ C.-H. Chen,^{59, 65} S. Chernichenko,²⁶ C.Y. Chi,¹⁴ J. Chiba,³⁴ M. Chiu,^{7, 27} I.J. Choi,^{27, 74} J.B. Choi,¹⁰ S. Choi,⁶³ R.K. Choudhury,⁴ P. Christiansen,⁴³ T. Chujo,^{69, 70} P. Chung,⁶⁴ A. Churyn,²⁶ O. Chvala,⁸ V. Cianciolo,⁵⁴ Z. Citron,^{65, 72} C.R. Cleven,²² B.A. Cole,¹⁴ M.P. Comets,⁵⁵ M. Connors,⁶⁵ P. Constantin,⁴¹ M. Csand,¹⁸ T. Csorgo,⁷³ T. Dahms,⁶⁵ S. Dairaku,^{37, 58} I. Danchev,⁷⁰ K. Das,²¹ A. Datta,^{45, 51} M.S. Daugherty,¹ G. David,⁷ M.B. Deaton,¹ K. DeBlasio,⁵¹ K. Dehmelt,^{20, 65} H. Delagrange,⁶⁶ A. Denisov,²⁶ D. d'Enterria,¹⁴ A. Deshpande,^{59, 65} E.J. Desmond,⁷ K.V. Dharmawardane,⁵² O. Dietzsch,⁶² L. Ding,³⁰ A. Dion,^{30, 65} J.H. Do,⁷⁴ M. Donadelli,⁶² O. Drapier,³⁸ A. Drees,⁶⁵ K.A. Drees,⁶ A.K. Dubey,⁷² J.M. Durham,^{41, 65} A. Durum,²⁶ D. Dutta,⁴ V. Dzhordzhadze,⁸ L. D'Orazio,⁴⁴ S. Edwards,^{6, 21} Y.V. Efremenko,⁵⁴ J. Egdemir,⁶⁵ F. Ellinghaus,¹³ W.S. Emam,⁸ T. Engelmore,¹⁴ A. Enokizono,^{40, 54, 58, 60} H. En'yo,^{58, 59} S. Esumi,⁶⁹ K.O. Eyser,⁸ B. Fadem,⁴⁸ N. Feege,⁶⁵ D.E. Fields,^{51, 59} M. Finger,^{9, 32} M. Finger, Jr.,^{9, 32} F. Fleuret,³⁸ S.L. Fokin,³⁶ Z. Fraenkel,^{72, *} J.E. Frantz,^{53, 65} A. Franz,⁷ A.D. Frawley,²¹ K. Fujiwara,⁵⁸ Y. Fukao,^{37, 58} T. Fusayasu,⁵⁰ S. Gadrat,⁴² K. Gainey,¹ C. Gal,⁶⁵ P. Gallus,¹⁵ P. Garg,³ A. Garishvili,⁶⁷ I. Garishvili,^{40, 67} H. Ge,⁶⁵ F. Giordano,²⁷ A. Glenn,^{13, 40} H. Gong,⁶⁵ X. Gong,⁶⁴ M. Gonin,³⁸ J. Gosset,¹⁶ Y. Goto,^{58, 59} R. Granier de Cassagnac,³⁸ N. Grau,^{2, 14, 30} S.V. Greene,⁷⁰ M. Grosser Perdekamp,^{27, 59} Y. Gu,⁶⁴ T. Gunji,¹² L. Guo,⁴¹ H. Guragain,²² H.-A. Gustafsson,^{43, *} T. Hachiya,^{24, 58} A. Hadj Henni,⁶⁶ C. Haegemann,⁵¹ J.S. Haggerty,⁷ K.I. Hahn,¹⁹ H. Hamagaki,¹² J. Hamblen,⁶⁷ R. Han,⁵⁶ S.Y. Han,¹⁹ J. Hanks,^{14, 65} H. Harada,²⁴ E.P. Hartouni,⁴⁰ K. Haruna,²⁴ S. Hasegawa,³¹ K. Hashimoto,^{58, 60} E. Haslum,⁴³ R. Hayano,¹² X. He,²² M. Heffner,⁴⁰ T.K. Hemmick,⁶⁵ T. Hester,⁸ H. Hiejima,²⁷ J.C. Hill,³⁰ R. Hobbs,⁵¹ M. Hohlmann,²⁰ R.S. Hollis,⁸ W. Holzmann,^{14, 64} K. Homma,²⁴ B. Hong,³⁵ T. Horaguchi,^{24, 58, 68, 69} Y. Hori,¹² D. Hornback,⁶⁷ T. Hoshino,²⁴ J. Huang,⁷ S. Huang,⁷⁰ T. Ichihara,^{58, 59} R. Ichimiya,⁵⁸ J. Ide,⁴⁸ H. Iinuma,^{34, 37, 58} Y. Ikeda,^{58, 69} K. Imai,^{31, 37, 58} Y. Imazu,⁵⁸ J. Imrek,¹⁷ M. Inaba,⁶⁹ Y. Inoue,^{58, 60} A. Iordanova,⁸ D. Isenhower,¹ L. Isenhower,¹ M. Ishihara,⁵⁸ T. Isobe,^{12, 58} M. Issah,^{64, 70} A. Isupov,³² D. Ivanischev,⁵⁷ D. Ivanishchev,⁵⁷ B.V. Jacak,⁶⁵ M. Javani,²² S.J. Jeon,⁴⁹ M. Jezghani,²² J. Jia,^{7, 14, 64} X. Jiang,⁴¹ J. Jin,¹⁴ O. Jinnouchi,⁵⁹ B.M. Johnson,⁷ E. Joo,³⁵ K.S. Joo,⁴⁹ D. Jouan,⁵⁵ D.S. Jumper,^{1, 27} F. Kajihara,¹² S. Kamei,^{12, 58, 71} N. Kamihara,^{58, 59} J. Kamin,⁶⁵ M. Kaneta,⁵⁹ S. Kaneti,⁶⁵ B.H. Kang,²³ J.H. Kang,⁷⁴ J.S. Kang,²³ H. Kanou,^{58, 68} J. Kapustinsky,⁴¹ K. Karatsu,^{37, 58} M. Kasai,^{58, 60} D. Kawall,^{45, 59} M. Kawashima,^{58, 60} A.V. Kazantsev,³⁶ T. Kempel,³⁰ J.A. Key,⁵¹ V. Khachatryan,⁶⁵ A. Khanzadeev,⁵⁷ K. Kihara,⁶⁹ K.M. Kijima,²⁴ J. Kikuchi,⁷¹ B.I. Kim,³⁵ C. Kim,³⁵ D.H. Kim,^{19, 49} D.J. Kim,^{33, 74} E. Kim,⁶³ E.-J. Kim,¹⁰ H.-J. Kim,⁷⁴ H.J. Kim,⁷⁴ K.-B. Kim,¹⁰ M. Kim,⁶³ S.H. Kim,⁷⁴ Y.-J. Kim,²⁷ Y.K. Kim,²³ E. Kinney,¹³ K. Kiriluk,¹³ A. Kiss,¹⁸ E. Kistenev,⁷ A. Kiyomichi,⁵⁸ J. Klatsky,²¹ J. Klay,⁴⁰ C. Klein-Boesing,⁴⁷ D. Kleinjan,⁸ P. Kline,⁶⁵ T. Koblesky,¹³ L. Kochenda,⁵⁷ V. Kochetkov,²⁶ M. Kofarago,¹⁸ Y. Komatsu,¹² B. Komkov,⁵⁷ M. Konno,⁶⁹ J. Koster,^{27, 59} D. Kotchetkov,^{8, 51, 53} D. Kotov,^{57, 61} A. Kozlov,⁷² A. Kral,¹⁵ A. Kravitz,¹⁴ F. Krizek,³³ J. Kubart,^{9, 29} G.J. Kunde,⁴¹ N. Kurihara,¹² K. Kurita,^{58, 60} M. Kurosawa,^{58, 59} M.J. Kweon,³⁵ Y. Kwon,^{67, 74} G.S. Kyle,⁵² R. Lacey,⁶⁴ Y.S. Lai,¹⁴ J.G. Lajoie,³⁰ A. Lebedev,³⁰ B. Lee,²³ D.M. Lee,⁴¹ J. Lee,¹⁹ K. Lee,⁶³ K.B. Lee,^{35, 41} K.S. Lee,³⁵ M.K. Lee,⁷⁴ S.H. Lee,⁶⁵ S.R. Lee,¹⁰ T. Lee,⁶³ M.J. Leitch,⁴¹ M.A.L. Leite,⁶² M. Leitgab,²⁷ E. Leitner,⁷⁰ B. Lenzi,⁶² B. Lewis,⁶⁵ X. Li,¹¹ P. Liebing,⁵⁹ S.H. Lim,⁷⁴ L.A. Linden Levy,¹³ T. Lika,¹⁵ A. Litvinenko,³² H. Liu,^{41, 52} M.X. Liu,⁴¹ B. Love,⁷⁰ R. Luechtenborg,⁴⁷ D. Lynch,⁷ C.F. Maguire,⁷⁰ Y.I. Makdisi,⁶ M. Makek,^{72, 75} A. Malakhov,³² M.D. Malik,⁵¹ A. Manion,⁶⁵ V.I. Manko,³⁶ E. Mannel,^{7, 14} Y. Mao,^{56, 58} L. Maek,^{9, 29} H. Masui,⁶⁹ S. Masumoto,¹² F. Matathias,¹⁴ M. McCumber,^{13, 41, 65} P.L. McGaughey,⁴¹ D. McGlinchey,^{13, 21} C. McKinney,²⁷ N. Means,⁶⁵ A. Meles,⁵² M. Mendoza,⁸ B. Meredith,^{14, 27} Y. Miake,⁶⁹ T. Mibe,³⁴ A.C. Mignerey,⁴⁴ P. Mike,^{9, 29} K. Miki,^{58, 69} A.J. Miller,¹

T.E. Miller,⁷⁰ A. Milov,^{7, 65, 72} S. Mioduszewski,⁷ D.K. Mishra,⁴ M. Mishra,³ J.T. Mitchell,⁷ M. Mitrovski,⁶⁴ Y. Miyachi,^{58, 68} S. Miyasaka,^{58, 68} S. Mizuno,^{58, 69} A.K. Mohanty,⁴ P. Montuenga,²⁷ H.J. Moon,⁴⁹ T. Moon,⁷⁴ Y. Morino,¹² A. Morreale,⁸ D.P. Morrison,^{7, †} S. Motschwiller,⁴⁸ T.V. Moukhanova,³⁶ D. Mukhopadhyay,⁷⁰ T. Murakami,^{37, 58} J. Murata,^{58, 60} A. Mwai,⁶⁴ T. Nagae,³⁷ S. Nagamiya,^{34, 58} Y. Nagata,⁶⁹ J.L. Nagle,^{13, ‡} M. Naglis,⁷² M.I. Nagy,^{18, 73} I. Nakagawa,^{58, 59} H. Nakagomi,^{58, 69} Y. Nakamiya,²⁴ K.R. Nakamura,^{37, 58} T. Nakamura,^{24, 34, 58} K. Nakano,^{58, 68} C. Nattrass,⁶⁷ A. Nederlof,⁴⁸ P.K. Netrakanti,⁴ J. Newby,⁴⁰ M. Nguyen,⁶⁵ M. Nihashi,^{24, 58} T. Niida,⁶⁹ B.E. Norman,⁴¹ R. Nouicer,^{7, 59} N. Novitzky,³³ A.S. Nyanin,³⁶ E. O'Brien,⁷ S.X. Oda,¹² C.A. Ogilvie,³⁰ H. Ohnishi,⁵⁸ M. Oka,⁶⁹ K. Okada,⁵⁹ O.O. Omiwade,¹ Y. Onuki,⁵⁸ J.D. Orjuela Koop,¹³ A. Oskarsson,⁴³ M. Ouchida,^{24, 58} H. Ozaki,⁶⁹ K. Ozawa,^{12, 34} R. Pak,⁷ D. Pal,⁷⁰ A.P.T. Palounek,⁴¹ V. Pantuev,^{28, 65} V. Papavassiliou,⁵² B.H. Park,²³ I.H. Park,¹⁹ J. Park,⁶³ S. Park,⁶³ S.K. Park,³⁵ W.J. Park,³⁵ S.F. Pate,⁵² L. Patel,²² M. Patel,³⁰ H. Pei,³⁰ J.-C. Peng,²⁷ H. Pereira,¹⁶ D.V. Perepelitsa,^{7, 14} G.D.N. Perera,⁵² V. Peresedov,³² D.Yu. Peressounko,³⁶ J. Perry,³⁰ R. Petti,⁶⁵ C. Pinkenburg,⁷ R. Pinson,¹ R.P. Pisani,⁷ M. Proissl,⁶⁵ M.L. Purschke,⁷ A.K. Purwar,⁴¹ H. Qu,^{1, 22} J. Rak,^{33, 51} A. Rakotozafindrabe,³⁸ I. Ravinovich,⁷² K.F. Read,^{54, 67} S. Rembeczki,²⁰ M. Reuter,⁶⁵ K. Reygers,⁴⁷ D. Reynolds,⁶⁴ V. Riabov,⁵⁷ Y. Riabov,^{57, 61} E. Richardson,⁴⁴ N. Rivelis,⁵³ D. Roach,⁷⁰ G. Roche,⁴² S.D. Rolnick,⁸ A. Romana,^{38, *} M. Rosati,³⁰ C.A. Rosen,¹³ S.S.E. Rosendahl,⁴³ P. Rosnet,⁴² Z. Rowan,⁵ J.G. Rubin,⁴⁶ P. Rukoyatkin,³² P. Ružička,²⁹ V.L. Rykov,⁵⁸ B. Sahlmueller,^{47, 65} N. Saito,^{34, 37, 58, 59} T. Sakaguchi,⁷ S. Sakai,⁶⁹ K. Sakashita,^{58, 68} H. Sakata,²⁴ H. Sako,³¹ V. Samsonov,⁵⁷ M. Sano,⁶⁹ S. Sano,^{12, 71} M. Sarsour,²² S. Sato,^{31, 34} T. Sato,⁶⁹ S. Sawada,³⁴ B. Schaefer,⁷⁰ B.K. Schmoll,⁶⁷ K. Sedgwick,⁸ J. Seele,^{13, 59} R. Seidl,^{27, 58, 59} A.Yu. Semenov,³⁰ V. Semenov,²⁶ A. Sen,^{22, 67} R. Seto,⁸ P. Sett,⁴ A. Sexton,⁴⁴ D. Sharma,^{65, 72} I. Shein,²⁶ A. Shevel,^{57, 64} T.-A. Shibata,^{58, 68} K. Shigaki,²⁴ M. Shimomura,^{30, 69} K. Shoji,^{37, 58} P. Shukla,⁴ A. Sickles,^{7, 65} C.L. Silva,^{30, 41, 62} D. Silvermyr,⁵⁴ C. Silvestre,¹⁶ K.S. Sim,³⁵ B.K. Singh,³ C.P. Singh,³ V. Singh,³ S. Skutnik,³⁰ M. Slunečka,^{9, 32} A. Soldatov,²⁶ R.A. Soltz,⁴⁰ W.E. Sondheim,⁴¹ S.P. Sorensen,⁶⁷ M. Soumya,⁶⁴ I.V. Sourikova,⁷ N.A. Sparks,¹ F. Staley,¹⁶ P.W. Stankus,⁵⁴ E. Stenlund,⁴³ M. Stepanov,^{45, 52} A. Ster,⁷³ S.P. Stoll,⁷ T. Sugitate,²⁴ C. Suire,⁵⁵ A. Sukhanov,⁷ T. Sumita,⁵⁸ J. Sun,⁶⁵ J. Szklai,⁷³ T. Tabaru,⁵⁹ S. Takagi,⁶⁹ E.M. Takagui,⁶² A. Takahara,¹² A. Taketani,^{58, 59} R. Tanabe,⁶⁹ Y. Tanaka,⁵⁰ S. Taneja,⁶⁵ K. Tanida,^{37, 58, 59, 63} M.J. Tannenbaum,⁷ S. Tarafdar,^{3, 72} A. Taranenko,⁶⁴ P. Tarján,¹⁷ E. Tennant,⁵² H. Themann,⁶⁵ T.L. Thomas,⁵¹ A. Timilsina,³⁰ T. Todoroki,^{58, 69} M. Togawa,^{37, 58} A. Toia,⁶⁵ J. Tojo,⁵⁸ L. Tomášek,²⁹ M. Tomášek,^{15, 29} H. Torii,^{12, 24, 58} M. Towell,¹ R. Towell,¹ R.S. Towell,¹ V-N. Tram,³⁸ I. Tserruya,⁷² Y. Tsuchimoto,^{12, 24} T. Tsuji,¹² C. Vale,^{7, 30} H. Valle,⁷⁰ H.W. van Hecke,⁴¹ M. Vargyas,^{18, 73} E. Vazquez-Zambrano,¹⁴ A. Veicht,^{14, 27} J. Velkovska,⁷⁰ R. Vértesi,^{17, 73} A.A. Vinogradov,³⁶ M. Virius,¹⁵ A. Vossen,²⁷ V. Vrba,^{15, 29} E. Vznuzdaev,⁵⁷ M. Wagner,^{37, 58} D. Walker,⁶⁵ X.R. Wang,⁵² D. Watanabe,²⁴ K. Watanabe,⁶⁹ Y. Watanabe,^{58, 59} Y.S. Watanabe,^{12, 34} F. Wei,^{30, 52} R. Wei,⁶⁴ J. Wessels,⁴⁷ S. Whitaker,³⁰ S.N. White,⁷ D. Winter,¹⁴ S. Wolin,²⁷ J.P. Wood,¹ C.L. Woody,⁷ R.M. Wright,¹ M. Wysocki,^{13, 54} B. Xia,⁵³ W. Xie,⁵⁹ L. Xue,²² S. Yalcin,⁶⁵ Y.L. Yamaguchi,^{12, 58, 71} K. Yamaura,²⁴ R. Yang,²⁷ A. Yanovich,²⁶ Z. Yasin,⁸ J. Ying,²² S. Yokkaichi,^{58, 59} I. Yoon,⁶³ Z. You,^{41, 56} G.R. Young,⁵⁴ I. Younus,^{39, 51} I.E. Yushmanov,³⁶ W.A. Zajc,¹⁴ O. Zaudtke,⁴⁷ A. Zelenski,⁶ C. Zhang,⁵⁴ S. Zhou,¹¹ J. Zimányi,^{73, *} and L. Zolin³²

(PHENIX Collaboration)

¹Abilene Christian University, Abilene, Texas 79699, USA

²Department of Physics, Augustana College, Sioux Falls, South Dakota 57197, USA

³Department of Physics, Banaras Hindu University, Varanasi 221005, India

⁴Bhabha Atomic Research Centre, Bombay 400 085, India

⁵Baruch College, City University of New York, New York, New York, 10010 USA

⁶Collider-Accelerator Department, Brookhaven National Laboratory, Upton, New York 11973-5000, USA

⁷Physics Department, Brookhaven National Laboratory, Upton, New York 11973-5000, USA

⁸University of California - Riverside, Riverside, California 92521, USA

⁹Charles University, Ovocný trh 5, Praha 1, 116 36, Prague, Czech Republic

¹⁰Chonbuk National University, Jeonju, 561-756, Korea

¹¹Science and Technology on Nuclear Data Laboratory, China Institute of Atomic Energy, Beijing 102413, People's Republic of China

¹²Center for Nuclear Study, Graduate School of Science, University of Tokyo, 7-3-1 Hongo, Bunkyo, Tokyo 113-0033, Japan

¹³University of Colorado, Boulder, Colorado 80309, USA

¹⁴Columbia University, New York, New York 10027 and Nevis Laboratories, Irvington, New York 10533, USA

¹⁵Czech Technical University, Zikova 4, 166 36 Prague 6, Czech Republic

¹⁶Dapnia, CEA Saclay, F-91191, Gif-sur-Yvette, France

¹⁷Debrecen University, H-4010 Debrecen, Egyetem tér 1, Hungary

¹⁸ELTE, Eötvös Loránd University, H-1117 Budapest, Pázmány Péter sétány 1/A, Hungary

- ¹⁹ Ewha Womans University, Seoul 120-750, Korea
²⁰ Florida Institute of Technology, Melbourne, Florida 32901, USA
²¹ Florida State University, Tallahassee, Florida 32306, USA
²² Georgia State University, Atlanta, Georgia 30303, USA
²³ Hanyang University, Seoul 133-792, Korea
²⁴ Hiroshima University, Kagamiyama, Higashi-Hiroshima 739-8526, Japan
²⁵ Department of Physics and Astronomy, Howard University, Washington, DC 20059, USA
²⁶ IHEP Protvino, State Research Center of Russian Federation, Institute for High Energy Physics, Protvino, 142281, Russia
²⁷ University of Illinois at Urbana-Champaign, Urbana, Illinois 61801, USA
²⁸ Institute for Nuclear Research of the Russian Academy of Sciences, prospekt 60-letiya Oktyabrya 7a, Moscow 117312, Russia
²⁹ Institute of Physics, Academy of Sciences of the Czech Republic, Na Slovance 2, 182 21 Prague 8, Czech Republic
³⁰ Iowa State University, Ames, Iowa 50011, USA
³¹ Advanced Science Research Center, Japan Atomic Energy Agency, 2-4 Shirakata Shirane, Tokai-mura, Naka-gun, Ibaraki-ken 319-1195, Japan
³² Joint Institute for Nuclear Research, 141980 Dubna, Moscow Region, Russia
³³ Helsinki Institute of Physics and University of Jyväskylä, P.O.Box 35, FI-40014 Jyväskylä, Finland
³⁴ KEK, High Energy Accelerator Research Organization, Tsukuba, Ibaraki 305-0801, Japan
³⁵ Korea University, Seoul, 136-701, Korea
³⁶ Russian Research Center "Kurchatov Institute," Moscow, 123098 Russia
³⁷ Kyoto University, Kyoto 606-8502, Japan
³⁸ Laboratoire Leprince-Ringuet, Ecole Polytechnique, CNRS-IN2P3, Route de Saclay, F-91128, Palaiseau, France
³⁹ Physics Department, Lahore University of Management Sciences, Lahore 54792, Pakistan
⁴⁰ Lawrence Livermore National Laboratory, Livermore, California 94550, USA
⁴¹ Los Alamos National Laboratory, Los Alamos, New Mexico 87545, USA
⁴² LPC, Université Blaise Pascal, CNRS-IN2P3, Clermont-Fd, 63177 Aubiere Cedex, France
⁴³ Department of Physics, Lund University, Box 118, SE-221 00 Lund, Sweden
⁴⁴ University of Maryland, College Park, Maryland 20742, USA
⁴⁵ Department of Physics, University of Massachusetts, Amherst, Massachusetts 01003-9337, USA
⁴⁶ Department of Physics, University of Michigan, Ann Arbor, Michigan 48109-1040, USA
⁴⁷ Institut für Kernphysik, University of Muenster, D-48149 Muenster, Germany
⁴⁸ Muhlenberg College, Allentown, Pennsylvania 18104-5586, USA
⁴⁹ Myongji University, Yongin, Kyonggido 449-728, Korea
⁵⁰ Nagasaki Institute of Applied Science, Nagasaki-shi, Nagasaki 851-0193, Japan
⁵¹ University of New Mexico, Albuquerque, New Mexico 87131, USA
⁵² New Mexico State University, Las Cruces, New Mexico 88003, USA
⁵³ Department of Physics and Astronomy, Ohio University, Athens, Ohio 45701, USA
⁵⁴ Oak Ridge National Laboratory, Oak Ridge, Tennessee 37831, USA
⁵⁵ IPN-Orsay, Universite Paris Sud, CNRS-IN2P3, BP1, F-91406, Orsay, France
⁵⁶ Peking University, Beijing 100871, People's Republic of China
⁵⁷ PNPI, Petersburg Nuclear Physics Institute, Gatchina, Leningrad Region, 188300, Russia
⁵⁸ RIKEN Nishina Center for Accelerator-Based Science, Wako, Saitama 351-0198, Japan
⁵⁹ RIKEN BNL Research Center, Brookhaven National Laboratory, Upton, New York 11973-5000, USA
⁶⁰ Physics Department, Rikkyo University, 3-34-1 Nishi-Ikebukuro, Toshima, Tokyo 171-8501, Japan
⁶¹ Saint Petersburg State Polytechnic University, St. Petersburg, 195251 Russia
⁶² Universidade de São Paulo, Instituto de Física, Caixa Postal 66318, São Paulo CEP05315-970, Brazil
⁶³ Department of Physics and Astronomy, Seoul National University, Seoul 151-742, Korea
⁶⁴ Chemistry Department, Stony Brook University, SUNY, Stony Brook, New York 11794-3400, USA
⁶⁵ Department of Physics and Astronomy, Stony Brook University, SUNY, Stony Brook, New York 11794-3800, USA
⁶⁶ SUBATECH (Ecole des Mines de Nantes, CNRS-IN2P3, Université de Nantes) BP 20722 - 44307, Nantes, France
⁶⁷ University of Tennessee, Knoxville, Tennessee 37996, USA
⁶⁸ Department of Physics, Tokyo Institute of Technology, Oh-okayama, Meguro, Tokyo 152-8551, Japan
⁶⁹ Institute of Physics, University of Tsukuba, Tsukuba, Ibaraki 305, Japan
⁷⁰ Vanderbilt University, Nashville, Tennessee 37235, USA
⁷¹ Waseda University, Advanced Research Institute for Science and Engineering, 17 Kikui-cho, Shinjuku-ku, Tokyo 162-0044, Japan
⁷² Weizmann Institute, Rehovot 76100, Israel
⁷³ Institute for Particle and Nuclear Physics, Wigner Research Centre for Physics, Hungarian Academy of Sciences (Wigner RCP, RMKI) H-1525 Budapest 114, POBox 49, Budapest, Hungary
⁷⁴ Yonsei University, IPAP, Seoul 120-749, Korea
⁷⁵ University of Zagreb, Faculty of Science, Department of Physics, Bijenička 32, HR-10002 Zagreb, Croatia

(Dated: August 13, 2019)

Two-pion interferometry measurements are used to extract the Gaussian radii R_{out} , R_{side} , and R_{long} , of the pion emission sources produced in Cu+Cu and Au+Au collisions at several beam collision energies $\sqrt{s_{NN}}$ at PHENIX. The extracted radii, which are compared to recent STAR and ALICE data, show characteristic scaling patterns as a function of the initial transverse size \bar{R} of the collision systems and the transverse mass m_T of the emitted pion pairs, consistent with hydrodynamiclike expansion. Specific combinations of the three-dimensional radii that are sensitive to the medium expansion velocity and lifetime, and the pion emission time duration show nonmonotonic $\sqrt{s_{NN}}$ dependencies. The nonmonotonic behaviors exhibited by these quantities point to a softening of the equation of state that may coincide with the critical end point in the phase diagram for nuclear matter.

PACS numbers: 25.75.Dw

Studies of the matter produced in ultrarelativistic heavy ion collisions provide an important avenue for mapping the phase diagram for quantum chromodynamics (QCD) [1–3]. Quantification of the properties of the various QCD phases, as well as pinpointing the location of the phase boundaries and the critical end point (CEP) in the plane of temperature vs. baryon chemical potential (T, μ_B) , are of fundamental interest [4].

Lattice QCD calculations indicate that the quark-hadron transition is a crossover at small μ_B or high collision energies ($\sqrt{s_{NN}}$) [5, 6]. Experimental results from the Relativistic Heavy Ion Collider (RHIC) at $\sqrt{s_{NN}} = 200$ GeV and the Large Hadron Collider (LHC) at $\sqrt{s_{NN}} = 2.76$ TeV, indicate that this transition results in the production of a strongly coupled plasma of deconfined quarks and gluons (sQGP) with low specific shear viscosity $\frac{\eta}{s}$, *i.e.* the ratio of shear viscosity η to entropy density s [7–14]. The validation of this crossover transition is a necessary, albeit insufficient, requirement for the existence of the CEP.

For lower beam energies or larger values of μ_B [15], model calculations [16–19] suggest that reaction trajectories in the (T, μ_B) -plane could come close to the CEP and even cross the coexistence curve that delineates a first order phase transition. Thus, a current strategy for experimental mapping of the phase diagram is centered on beam energy scans, which sample reaction trajectories with the broadest possible range of μ_B and T values.

The expansion dynamics of the matter produced in these beam energy scans is strongly influenced by the reaction trajectory in the (T, μ_B) -plane. At the CEP or close to it, anomalies in the dynamic properties of the medium can drive abrupt changes in transport coefficients and relaxation rates to give a nonmonotonic dependence of $\frac{\eta}{s}(T, \mu_B)$ [11, 20, 21]. A medium produced in the vicinity of the CEP could also show a stalling of the mean expansion speed, c_s [22, 23], as well as a longer emission duration $\Delta\tau$, manifested as a difference between R_{out} and R_{side} ($\Delta\tau^2 \propto (R_{\text{out}}^2 - R_{\text{side}}^2)$) [22–26]. Here, the rationale is that, in the vicinity of the CEP, the equation of state (EOS) “softens” considerably and this could cause the expansion to stall and prolong the emission duration to give $R_{\text{out}} > R_{\text{side}}$.

In a recent study, the acoustic scaling properties of

collective flow were used to extract viscous coefficients as a function of $\sqrt{s_{NN}}$ [27]. A striking pattern of viscous damping, compatible with the expected minimum of $\frac{\eta}{s}(T, \mu_B)$ for trajectories in the vicinity of the CEP [20, 21], was reported. Such trajectories should also lead to signatures indicative of a softening of the EOS and a prolonged emission duration. Both can influence the space-time extent to give a measurable nonmonotonic $\sqrt{s_{NN}}$ dependence of the medium expansion velocity and the duration of particle emission.

In this Letter, we use the interferometry technique of Hanbury Brown and Twiss (HBT) [28] to perform detailed differential measurements of two-pion correlation functions [24, 29–36] in Cu+Cu collisions at $\sqrt{s_{NN}} = 200$ GeV and Au+Au collisions at $\sqrt{s_{NN}} = 39.0, 62.4$, and 200 GeV. The correlation functions are then used to extract and compare the emission source radii to similar measurements for Au+Au collisions ($\sqrt{s_{NN}} = 7–200$ GeV) by the STAR collaboration [37] and Pb+Pb collisions ($\sqrt{s_{NN}} = 2.76$ TeV) by the ALICE collaboration at the LHC [35]. We test the scaling properties of specific combinations of the 3D radii that are sensitive to the expansion velocity (and thus also the speed of sound) and the emission time duration, which allow a search for their possible nonmonotonic dependence on $\sqrt{s_{NN}}$.

The present analysis uses the data recorded by the PHENIX experiment for Cu+Cu collisions during the 2005 RHIC running period and for Au+Au collisions during the 2007 and 2010 running periods. Event triggering, as well as determination of the collision vertex z (along the beam axis) was obtained with the Beam-Beam Counters located on either side of the interaction point of PHENIX. This vertex was constrained to $|z| < 30$ cm. The charge distribution measured in the beam-beam counters, which span the pseudorapidity range $3.0 < |\eta| < 3.9$ [38]. Track and momentum reconstruction for charged particles were performed by combining hits from the drift chambers (DC) and pad chambers in the PHENIX central spectrometers ($|\eta| < 0.35$). Charged pions were identified by combining time-of-flight from the two time-of-flight detectors, as well as the electromagnetic calorimeters [39], with momentum reconstructed from the DC and pad-chamber hits in the magnetic field. Particles within 2 standard deviations of the

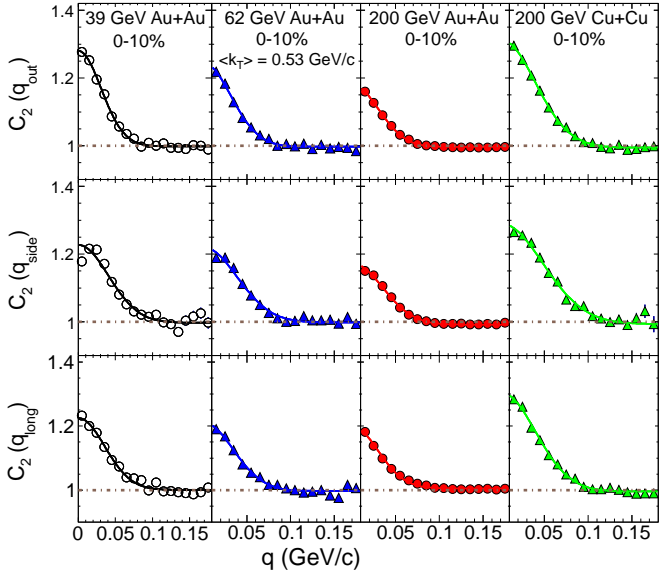


FIG. 1. (Color online) Slices of the 3D two-pion ($\pi^+\pi^+$ and $\pi^-\pi^-$) correlation functions for 0%–10% central Au+Au (left panels) and Cu+Cu (rightmost panel) collisions for $\langle k_T \rangle = 0.53$ GeV/c and for several beam collision energies as indicated. The curves represent fits to the correlation function (see text).

peak for charged pions in the squared mass distribution were identified as pions for momenta up to ~ 1 GeV/c as detailed in Ref. [38].

The two-pion correlation function is defined as the ratio $C_2(\mathbf{q}) = A(\mathbf{q})/B(\mathbf{q})$, where $A(\mathbf{q})$ is the measured distribution of the relative momentum difference $\mathbf{q} = \mathbf{p}_2 - \mathbf{p}_1$ between particle pairs with momenta \mathbf{p}_1 and \mathbf{p}_2 ; $B(\mathbf{q})$ is the uncorrelated distribution, obtained from particle pairs in which each particle is selected from a different event but with similar event centralities, vertex positions, and charge sign. The effects of track merging and track splitting [31, 34] were suppressed via pair selection cuts in the DC and the electromagnetic calorimeters, as detailed in Ref. [34]. The relative momentum \mathbf{q} is calculated in the longitudinally co-moving system, where the longitudinal pair momentum (along the beam direction) is zero. It is also decomposed into its three components, q_{out} , q_{side} , and q_{long} , following the Bertsch-Pratt convention [40, 41], *i.e.* the “out” axis points along the pair transverse momentum, the “side” axis is perpendicular to the out axis, and the “long” axis points along the beam.

Correlation functions were studied as a function of collision centrality, as well as for different pion-pair transverse momenta $k_T = |\mathbf{p}_{T,1} + \mathbf{p}_{T,2}|/2$ or transverse mass $m_T = \sqrt{(k_T^2 + m_\pi^2)}$, where m_π is the pion mass. Figure 1 shows a representative set of plots from the three-dimensional two-pion correlation functions for central (0%–10%) Au+Au and Cu+Cu collisions for $\langle k_T \rangle = 0.53$ GeV/c for several values of $\sqrt{s_{NN}}$. The plots all

show the familiar Bose-Einstein enhancement peak at low q . The larger peak widths for Cu+Cu reflects the difference in the initial geometric sizes for 0%–10% central Cu+Cu and Au+Au collisions.

Correlation functions were extracted for a detailed set of centrality and m_T cuts, to allow a study of the emission sources as a function of pair momentum and initial-state transverse size characterized as follows. In a Monte Carlo Glauber (MC-Glauber) calculation [42–44] a subset of the nucleons become participants (N_{part}) in each collision by undergoing an initial inelastic N+N interaction. The transverse distribution of these participants in the X-Y plane has RMS widths σ_x and σ_y along its principal axes. We define \bar{R} , the characteristic initial transverse size, as $1/\bar{R} = \sqrt{(1/\sigma_x^2 + 1/\sigma_y^2)}$ [45]. The \bar{R} and N_{part} were computed as a function of collision centrality. Note that, for central collisions, the initial Gaussian radius for the collision system $R \approx \sqrt{2}\bar{R}$. The systematic uncertainties for these geometric quantities, obtained via variation of the model parameters, are less than 10% [44].

The correlation functions were fitted with the following expression (in which cross-terms are assumed to be negligible) which accounts for the Bose-Einstein enhancement and the Coulomb interaction between pion pairs [46, 47]:

$$C_2(\mathbf{q}) = N[(\lambda(1 + G(\mathbf{q})))F_c + (1 - \lambda)], \\ G(\mathbf{q}) \cong \exp(-R_{\text{side}}^2 q_{\text{side}}^2 - R_{\text{out}}^2 q_{\text{out}}^2 - R_{\text{long}}^2 q_{\text{long}}^2), \quad (1)$$

where N is a normalization factor, λ is the correlation strength, F_c is the Coulomb correction factor [47] evaluated with the Coulomb wave function, and R_{out} , R_{side} and R_{long} are the Gaussian HBT radii which characterize the emission source. R_{long} is related to medium lifetime and $(R_{\text{out}}^2 - R_{\text{side}}^2)$ is sensitive to $\Delta\tau$ [25, 26]. Similarly, $(R_{\text{side}} - \sqrt{2}\bar{R})$ gives an estimate for the expansion radius for small values of m_T .

Good fits to the correlation functions for the Cu+Cu and Au+Au systems were obtained (cf. Fig. 1) and cross-checked to confirm agreement with our earlier measurements for Au+Au collisions [31, 34, 48]. The fit parameters for $\pi^+\pi^+$ and $\pi^-\pi^-$ pairs were also found to agree within statistical uncertainties; the data for $\pi^+\pi^+$ and $\pi^-\pi^-$ were therefore combined. The systematic uncertainties for the fits were estimated via variations of the cuts used to generate the correlation functions (single track cuts, pair selection cuts and particle identification cuts). Typical values of the systematic uncertainties for R_{out} , R_{side} , and R_{long} are 5% and do not exceed 8%.

At freeze-out, the space-time extent of an emission source reflects its initial size, its growth in size over the duration of its lifetime or expansion time τ , as well as a diminution in size with m_T , due to position-momentum correlations. The expansion time $\tau \propto \bar{R}$ [27, 50, 51]. Therefore, R_{out} , R_{side} , and R_{long} might be expected to scale with \bar{R} for a given m_T . Position-momentum correlations reduce the magnitude of these radii [31, 32, 35],

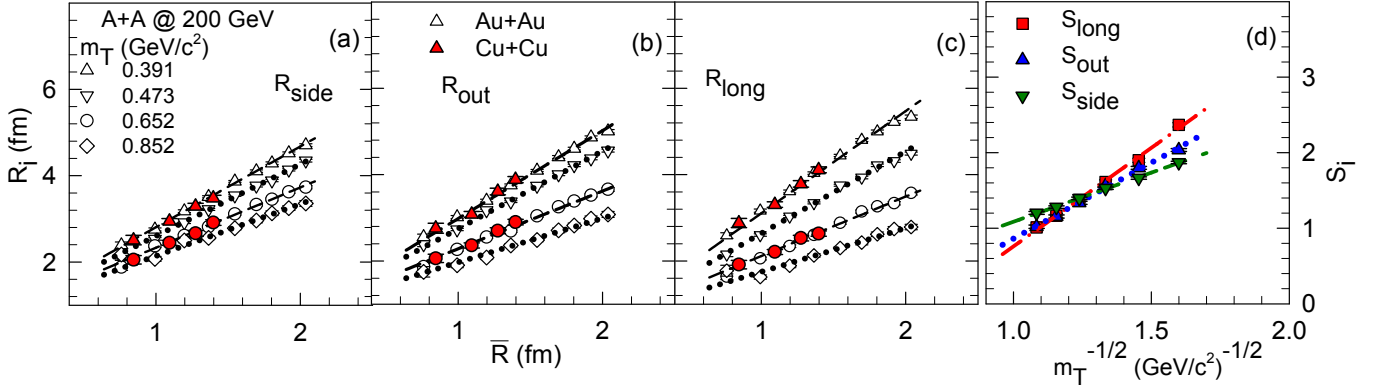


FIG. 2. (Color online) HBT radii vs. \bar{R} for several m_T cuts (as indicated) for (a) R_{side} , (b) R_{out} and (c) R_{long} for 0%–10%, 10%–20%, 20%–30% and 30%–40% Cu+Cu collisions, and 0%–5%, 5–10%, 10%–15%, 15–20%, 20%–30%, 30%–40%, 40%–50%, 50%–60% and 60%–70% Au+Au collisions at $\sqrt{s_{NN}} = 200$ GeV. (d) S_i vs. $1/\sqrt{m_T}$; S_i are slopes obtained from the respective linear fits to R_{side} , R_{out} , and R_{long} vs. \bar{R} , shown in (a), (b) and (c). The curves in (a)–(d) represent linear fits.

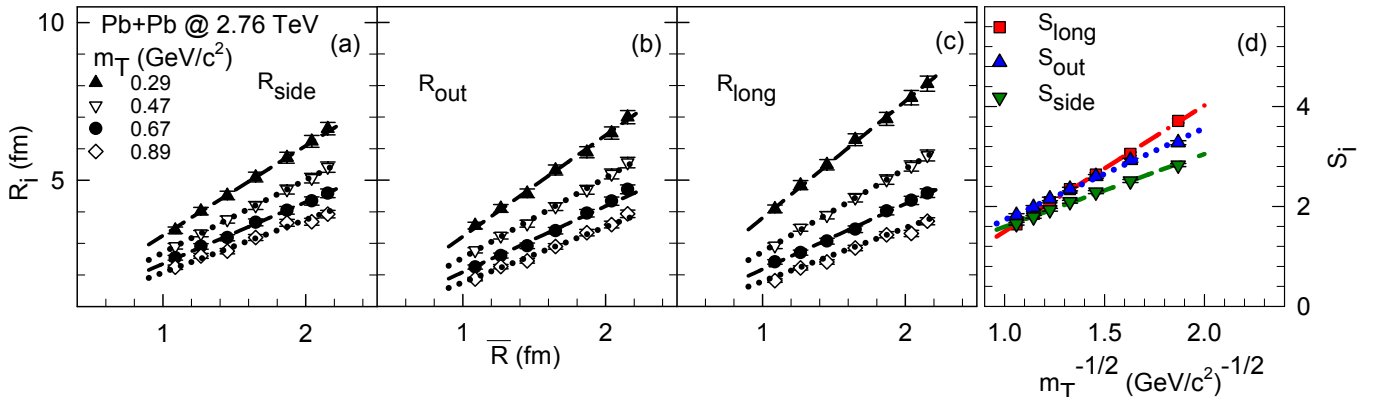


FIG. 3. (Color online) Same as Fig. 2, but for Pb+Pb collisions at $\sqrt{s_{NN}} = 2.76$ TeV; the data are taken from Ref. [49].

so it is instructive to investigate m_T scaling as well.

Figure 2 gives a summary of the detailed centrality and m_T dependence of the extracted radii for Cu+Cu and Au+Au collisions at $\sqrt{s_{NN}} = 200$ GeV. Figures 2(a), (b) and (c) validate the expected linear dependence of R_{side} , R_{out} and R_{long} on \bar{R} for both systems and show that the magnitudes of the radii for each system, are comparable at similar values of \bar{R} and m_T . They also indicate the expected decrease in the slope of the respective scaling curves (for R_{side} , R_{out} , and R_{long}) with m_T . The latter confirms the important influence of position-momentum correlations which result from collective expansion in the Cu+Cu and Au+Au systems. Similar scaling patterns were observed for the full range of $\sqrt{s_{NN}}$ values spanned by the STAR data set [37].

Figures 3(a), (b) and (c) show that the same scaling patterns are also observed for the HBT radii extracted in Pb+Pb collisions at $\sqrt{s_{NN}} = 2.76$ TeV, albeit with

significantly larger magnitudes for R_{side} , R_{out} , and R_{long} . Because the values for \bar{R} in Pb+Pb collisions are only $\sim 5\%$ larger than those for Au+Au collisions, the larger radii observed at $\sqrt{s_{NN}} = 2.76$ TeV could be the result of an increase in the total system lifetime and/or a larger expansion velocity from RHIC to the LHC.

Linear fits were made to the plots of the HBT radii vs. \bar{R} for the full range of m_T selections [cf. dashed and dotted curves in Figs. 2 and 3 (a)–(c)], to gain further insights on the m_T dependence of the position-momentum correlations. Figures 2(d) and 3(d) show that the slopes S_i obtained from these linear fits, scale as $1/\sqrt{m_T}$ and the position-momentum correlations are largest (smallest) in the long (side) direction. They also indicate that, for a given $\sqrt{s_{NN}}$, the full set of differential measurements for each radius, can be made to scale to a single curve.

Figure 4 shows a further demonstration of these scaling patterns for PHENIX and STAR measurements for

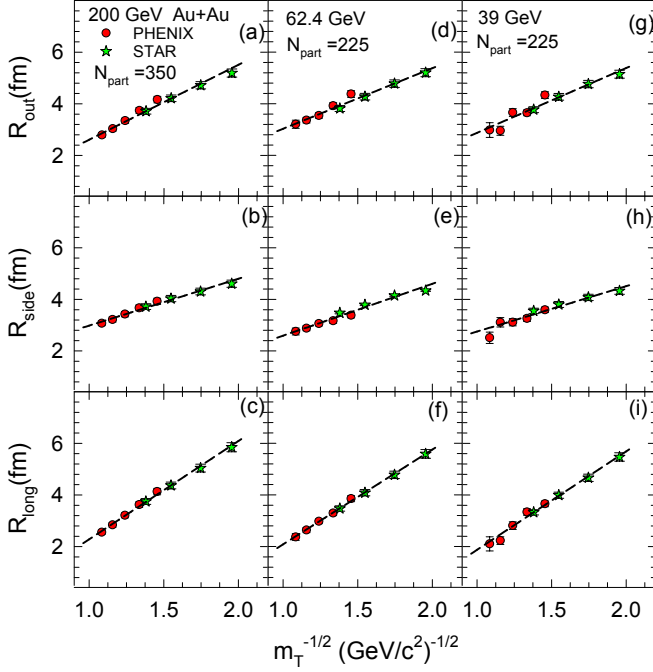


FIG. 4. (Color online) Comparison of PHENIX and STAR HBT radii for Au+Au collisions at $\sqrt{s_{NN}} = 39.0, 62.4$ and 200 GeV as indicated. The STAR data are taken from Ref. [37]. The data points represent the results from fits to the m_T dependence of the combined data sets.

Au+Au collisions at $\sqrt{s_{NN}} = 39, 62.4$ and 200 GeV. The results for two centrality or N_{part} selections indicate the characteristic $1/\sqrt{m_T}$ dependence of R_{out} , R_{side} , and R_{long} for each beam energy presented. They also indicate good agreement between the PHENIX and STAR data sets. The PHENIX data provide a sizable extension to the m_T reach of the available data for HBT radii at RHIC. Similar scaling was observed for the full range of $\sqrt{s_{NN}}$ measurements spanned by the ALICE and STAR data sets [37, 49].

The quantities $(R_{\text{out}}^2 - R_{\text{side}}^2)$ and $[(R_{\text{side}} - \sqrt{2}\bar{R})/R_{\text{long}}]$ were obtained at $m_T = 0.26$ GeV/ c^2 to reduce the effects of position-momentum correlations. These quantities, which are related to the emission duration and expansion velocity respectively, were investigated as a function of $\sqrt{s_{NN}}$. Figures 5(a) and (b) show these dependencies for the 5% most central collisions of the combined data sets. Similar patterns were observed for other m_T selections, albeit with different magnitudes. These nonmonotonic patterns are consistent with the minimum observed for the $\sqrt{s_{NN}}$ dependence of the viscous coefficients reported in Ref. [27], and could be a further indication of trajectories passing through the softest region in the equation of state and possibly the CEP.

In summary, we have presented new PHENIX measurements of two-pion interferometry and used them to extract the Gaussian source radii R_{out} , R_{side} , and R_{long} , of the emission sources produced in Cu+Cu and Au+Au

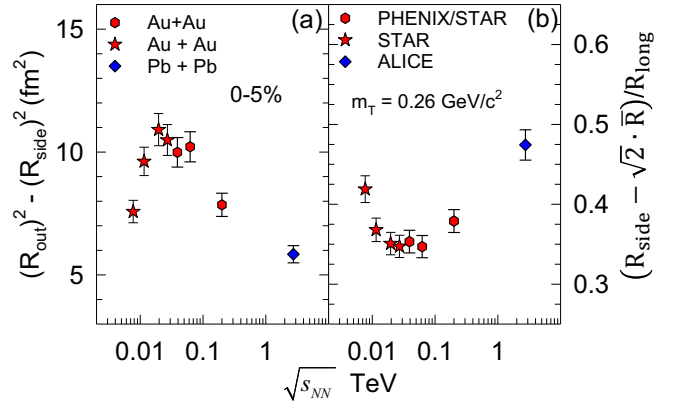


FIG. 5. (Color online) The $\sqrt{s_{NN}}$ dependence of (a) $(R_{\text{out}}^2 - R_{\text{side}}^2)$, (b) $[(R_{\text{side}} - \sqrt{2}\bar{R})/R_{\text{long}}]$. The HBT radii are taken from the present work and Refs. [37, 49]. The PHENIX and STAR data points represent the results from fits to the m_T dependence of the combined data sets.

collisions at several beam energies. The extracted HBT radii, which are compared to recent STAR and ALICE data, exhibit characteristic scaling patterns as a function of m_T and \bar{R} which allow an investigation of the $\sqrt{s_{NN}}$ dependence of the quantities $R_{\text{out}}^2 - R_{\text{side}}^2$ and $R_{\text{side}} - \sqrt{2}\bar{R}/R_{\text{long}}$ which are sensitive to the emission duration and expansion velocity, respectively. Non-monotonic dependencies observed in these variables may be linked to trajectories that spend a significant fraction of time near the softest point in the equation of state and possibly the CEP. Further detailed studies are required to make a more precise mapping, as well as to confirm that the observed patterns are linked to trajectories close to the critical end point in the phase diagram for nuclear matter.

We thank the staff of the Collider-Accelerator and Physics Departments at Brookhaven National Laboratory and the staff of the other PHENIX participating institutions for their vital contributions. We acknowledge support from the Office of Nuclear Physics in the Office of Science of the Department of Energy, the National Science Foundation, Abilene Christian University Research Council, Research Foundation of SUNY, and Dean of the College of Arts and Sciences, Vanderbilt University (U.S.A), Ministry of Education, Culture, Sports, Science, and Technology and the Japan Society for the Promotion of Science (Japan), Conselho Nacional de Desenvolvimento Científico e Tecnológico and Fundação de Amparo à Pesquisa do Estado de São Paulo (Brazil), Natural Science Foundation of China (P. R. China), Ministry of Science, Education, and Sports (Croatia), Ministry of Education, Youth and Sports (Czech Republic), Centre National de la Recherche Scientifique, Commissariat à l'Énergie Atomique, and Institut National de Physique Nucléaire et de Physique des Particules

(France), Bundesministerium für Bildung und Forschung, Deutscher Akademischer Austausch Dienst, and Alexander von Humboldt Stiftung (Germany), OTKA NK 101428 grant and the Ch. Simonyi Fund (Hungary), Department of Atomic Energy and Department of Science and Technology (India), Israel Science Foundation (Israel), Basic Science Research Program through NRF of the Ministry of Education (Korea), Physics Department, Lahore University of Management Sciences (Pakistan), Ministry of Education and Science, Russian Academy of Sciences, Federal Agency of Atomic Energy (Russia), VR and Wallenberg Foundation (Sweden), the U.S. Civilian Research and Development Foundation for the Independent States of the Former Soviet Union, the Hungarian American Enterprise Scholarship Fund, and the US-Israel Binational Science Foundation.

Rev. Lett. **97**, 152303 (2006).

- [21] R. A. Lacey, N. N. Ajitanand, J. M. Alexander, P. Chung, J. Jia, and A. Taranenko, arXiv:0708.3512.
- [22] C. M. Hung and E. V. Shuryak, Phys. Rev. Lett. **75**, 4003 (1995).
- [23] D. H. Rischke and M. Gyulassy, Nucl. Phys. A **608**, 479 (1996).
- [24] S. Pratt, Phys. Rev. Lett. **53**, 1219 (1984).
- [25] S. Chapman, P. Scotto, and U. W. Heinz, Phys. Rev. Lett. **74**, 4400 (1995).
- [26] U. A. Wiedemann, P. Scotto, and U. W. Heinz, Phys. Rev. C **53**, 918 (1996).
- [27] R. A. Lacey, A. Taranenko, J. Jia, D. Reynolds, N. N. Ajitanand, J. M. Alexander, Y. Gu, and A. Mwai, Phys. Rev. Lett. **112**, 082302 (2014).
- [28] R. H. Brown and R. Q. Twiss, Nature **178**, 1046 (1956).
- [29] W. Zajc, J. Bistirlich, R. Bossingham, H. Bowman, C. Clawson, *et al.*, Phys. Rev. C **29**, 2173 (1984).
- [30] R. Ganz *et al.* (NA49 Collaboration), arXiv:nucl-ex/9808006.
- [31] S. Adler *et al.* (PHENIX Collaboration), Phys. Rev. Lett. **93**, 152302 (2004).
- [32] J. Adams *et al.* (STAR Collaboration), Phys. Rev. C **71**, 044906 (2005).
- [33] M. A. Lisa, S. Pratt, R. Soltz, and U. Wiedemann, Ann. Rev. Nucl. Part. Sci. **55**, 357 (2005).
- [34] S. Afanasiev *et al.* (PHENIX Collaboration), Phys. Rev. Lett. **100**, 232301 (2008).
- [35] K. Aamodt *et al.* (ALICE Collaboration), Phys. Lett. B **696**, 328 (2011).
- [36] A. Adare *et al.* (PHENIX Collaboration), Phys. Rev. Lett. **112**, 222301 (2014).
- [37] L. Adamczyk *et al.* (STAR Collaboration), arXiv:1403.4972.
- [38] A. Adare *et al.* (PHENIX Collaboration), Phys. Rev. C **88**, 024906 (2013).
- [39] L. Aphecetche *et al.* (PHENIX Collaboration), Nucl. Instrum. Methods A **499**, 521 (2003).
- [40] G. Bertsch, Nucl. Phys. A **498**, 173C (1989).
- [41] S. Pratt, Phys. Rev. D **33**, 1314 (1986).
- [42] M. L. Miller, K. Reygers, S. J. Sanders, and P. Steinberg, Ann. Rev. Nucl. Part. Sci. **57**, 205 (2007).
- [43] R. A. Lacey, R. Wei, J. Jia, N. N. Ajitanand, J. M. Alexander, and A. Taranenko, Phys. Rev. C **83**, 044902 (2011).
- [44] A. Adare *et al.* (PHENIX Collaboration), arXiv:1310.4793.
- [45] R. Bhalerao, J.-P. Blaizot, N. Borghini, and J.-Y. Ollitrault, Phys. Lett. B **627**, 49 (2005).
- [46] M. G. Bowler, Phys. Lett. B **270**, 69 (1991).
- [47] Y. Sinyukov, R. Lednický, S. Akkelin, J. Pluta, and B. Erazmus, Phys. Lett. B **432**, 248 (1998).
- [48] A. Adare *et al.* (PHENIX Collaboration), arXiv:1404.5291.
- [49] A. Kisiel (ALICE Collaboration), Proc. Sci. **WPCF2011**, 003 (2011).
- [50] R. A. Lacey, Y. Gu, X. Gong, D. Reynolds, N. N. Ajitanand, J. M. Alexander, A. Mwai, and A. Taranenko, arXiv:1301.0165.
- [51] E. Shuryak and I. Zahed, Phys. Rev. C **88**, 044915 (2013).
- [52] J. Cleymans, H. Oeschler, K. Redlich, and S. Wheaton, J. Phys. G **32**, S165 (2006).